

DESY 10-203
Edinburgh 2010/31
LTH 890

Hyperon Form Factors from $N_f = 2 + 1$ QCD

**M. Göckeler^a, Ph. Hägler^a, R. Horsley^b, Y. Nakamura^{a,c}, D. Pleiter^d, P. E. L. Rakow^e,
A. Schäfer^a, G. Schierholz^d, H. Stüben^f, F. Winter^a, J. M. Zanotti^{*,b}**

^a *Institut für Theoretische Physik, Universität Regensburg, 93040 Regensburg, Germany*

^b *School of Physics and Astronomy, University of Edinburgh, Edinburgh EH9 3JZ, UK*

^c *Center for Computational Sciences, University of Tsukuba, Tsukuba, Ibaraki 305-8577, Japan[†]*

^d *Deutsches Elektronen-Synchrotron DESY, 15738 Zeuthen, Germany*

^e *Theoretical Physics Division, Department of Mathematical Sciences, University of Liverpool,
Liverpool L69 3BX, UK*

^f *Konrad-Zuse-Zentrum für Informationstechnik Berlin, 14195 Berlin, Germany*

E-mail: jzanotti@ph.ed.ac.uk

QCDSF/UKQCD Collaboration

We present results from the QCDSF/UKQCD collaboration for the electromagnetic and semi-leptonic form factors for the hyperons. The simulations are performed on our new ensembles generated with 2+1 flavours of dynamical $\mathcal{O}(a)$ -improved Wilson fermions. A unique feature of these configurations is that the quark masses are tuned so that the singlet quark mass is held fixed at its physical value. We use 5 such choices of the individual quark masses on $24^3 \times 48$ lattices with a lattice spacing of about 0.078 fm.

*The XXVIII International Symposium on Lattice Field Theory, Lattice2010
June 14-19, 2010
Villasimius, Italy*

*Speaker.

[†]present address

1. Introduction

The study of the electromagnetic (EM) properties of hadrons provides important insights into the non-perturbative structure of QCD. The EM form factors reveal information on the internal structure of hadrons including their size, charge distribution and magnetisation.

While the EM form factors of the nucleon have received a lot of recent attention in lattice simulations (see, e.g., [1] for a review), the investigation of the hyperon EM form factors has so far received only limited attention [2, 3]. These, however, are of significant interest as they provide valuable insights into the environmental sensitivity of the distribution of quarks inside a hadron. For example, how does the distribution of u quarks in Σ^+ change as we change the mass of the (spectator) s quark?

Semileptonic form factors of the hyperons provide an alternative method to the standard $K_{\ell 3}$ decays (see e.g. [4]) for determining the CKM matrix element, $|V_{us}|$. This is done by using the experimental value for the decay rate of the hyperon beta decays, $B \rightarrow b\ell\nu$

$$\Gamma = \frac{G_F^2}{60\pi^3} (M_B - M_b)^5 (1 - 3\delta) |V_{us}|^2 |f_1(0)|^2 \left(1 + 3 \left| \frac{g_1(0)}{f_1(0)} \right|^2 + \dots \right), \quad (1.1)$$

where G_F is the Fermi constant, $\delta = (M_B - M_b)/(M_B + M_b)$ describes the size of $SU(3)_{\text{flavour}}$ breaking and the ellipsis denotes terms which are $\mathcal{O}(\delta^2)$ and can be safely ignored [5]. Hence for a determination of $|V_{us}|$, we need to know the form factors, $f_1(q^2)$ and $g_1(q^2)$, at zero momentum transfer ($q^2 = 0$). These can be determined on the lattice and are the subject of the second part of this talk. Earlier quenched and $N_f = 2$ results for $\Sigma^- \rightarrow n\ell\nu$ and $\Xi^0 \rightarrow \Sigma^+\ell\nu$ can be found in [6, 7].

In this talk we present preliminary results from the QCDSF/UKQCD Collaboration for the octet hyperon electromagnetic and semi-leptonic decay form factors determined from $N_f = 2 + 1$ lattice QCD.

2. Simulation Details

Our gauge field configurations have been generated with $N_f = 2 + 1$ flavours of dynamical fermions, using the tree-level Symanzik improved gluon action and nonperturbatively $\mathcal{O}(a)$ improved Wilson fermions [8]. We choose our quark masses by first finding the $SU(3)_{\text{flavour}}$ -symmetric point where flavour singlet quantities take on their physical values and vary the individual quark masses while keeping the singlet quark mass $\bar{m}_q = (m_u + m_d + m_s)/3 = (2m_l + m_s)/3$ constant [9]. Simulations are performed on lattice volumes of $24^3 \times 48$ with lattice spacing, $a = 0.078(3)$. A summary of the parameter space spanned by our dynamical configurations can be found in Table 1. More details regarding the tuning of our simulation parameters are given in Ref. [9].

3. Electromagnetic Form Factors

On the lattice, we determine the form factors $F_1(q^2)$ and $F_2(q^2)$ by calculating the following matrix element of the electromagnetic current

$$\langle B(p', s') | j_\mu(q) | B(p, s) \rangle = \bar{u}(p', s') \left[\gamma_\mu F_1(q^2) + \sigma_{\mu\nu} \frac{q_\nu}{2M_B} F_2(q^2) \right] u(p, s), \quad (3.1)$$

Ensemble	κ_l	κ_s	m_π [MeV]	m_K [MeV]	m_N [GeV]	m_Σ [GeV]	m_Ξ [GeV]
1	0.12083	0.12104	481	420	1.257	1.209	1.180
2	0.12090	0.12090	443	443	1.231	1.231	1.231
3	0.12095	0.12080	414	459	1.205	1.240	1.258
4	0.12100	0.12070	377	473	1.175	1.242	1.278
5	0.12104	0.12062	350	485	1.123	1.222	1.280

Table 1: Pion, Kaon and octet baryon masses on $24^3 \times 48$ lattices with lattice spacing, $a = 0.078(3)$ fm

where $u(p, s)$ is a Dirac spinor with momentum, p , and spin polarisation, s , $q = p' - p$ is the momentum transfer, M_B is the mass of the baryon, B , and j_μ is the electromagnetic current. The Dirac (F_1) and Pauli (F_2) form factors of the proton are obtained by using $j_\mu^{(p)} = \frac{2}{3}\bar{u}\gamma_\mu u - \frac{1}{3}\bar{d}\gamma_\mu d$, while the form factors for the Σ and Ξ baryons are obtained through the appropriate substitution, $u \rightarrow s$ or $d \rightarrow s$. It is common to rewrite the form factors F_1 and F_2 in terms of the electric and magnetic Sachs form factors, $G_e = F_1 + q^2/(2M_N)^2 F_2$ and $G_m = F_1 + F_2$.

If one is using a conserved current, then (e.g. for the proton) $F_1^{(p)}(0) = G_e^{(p)}(0) = 1$ gives the electric charge, while $G_m^{(p)}(0) = \mu^{(p)} = 1 + \kappa^{(p)}$ gives the magnetic moment, where $F_2^{(p)}(0) = \kappa^{(p)}$ is the anomalous magnetic moment. From Eq. (3.1) we see that F_2 always appears with a factor of q , so it is not possible to extract a value for F_2 at $q^2 = 0$ directly from our lattice simulations. Hence we are required to extrapolate the results we obtain at finite q^2 to $q^2 = 0$. Form factor radii, $r_i = \sqrt{\langle r_i^2 \rangle}$, are defined from the slope of the form factor at $q^2 = 0$.

In this talk, we are primarily interested in searching for any $SU(3)$ -flavour breaking effects in the octet hyperon form factors. In order to highlight these effects, we will consider ratios of the individual quark contributions to the hyperon radii. For example, the ratio $\langle r_1^2 \rangle_{u_\Sigma} / \langle r_1^2 \rangle_{u_p}$ will tell us about the distribution of the doubly represented (u -)quark in a baryon as we change the doubly-singly represented quark mass splitting (in effect, changing the mass of the spectator quark).

In Fig. 1 we see results for the ratio of the doubly-represented quark's contribution to the Dirac radius of the hyperons plotted as a function of m_π^2 . Here we clearly see that the Dirac radii, $\langle r_1^2 \rangle$, of both $u(d)$ -quark in the $\Sigma^{+(-)}$ and the s -quark in the $\Xi^{0/-}$ become smaller than that of the u -quark in the proton as we move away from the $SU(3)_{\text{flavour}}$ symmetric point by decreasing (increasing) the light (strange) quark mass. This is particularly interesting in the case of u_Σ , since here the only difference between u_Σ and u_p is the mass of the spectator quark ($d(u)$ in the proton (neutron), s in the Σ), so the fact that the ratio is < 1 is a purely environmental effect.

In Fig. 2 we see a similar picture for the distribution of the singly represented quarks with the $d(u)$ -quark in the proton (neutron) having a larger Dirac radius than the $u(d)$ -quark in the $\Xi^{0(-)}$ and the s -quark in the Σ having the smallest Dirac radius.

These effects are similar to those seen in an earlier quenched QCD simulation [2], however here the effects are slightly enhanced due to the fact that the strength of the meson loops is suppressed in quenched QCD [10].

Similar results are found for $\langle r_2^2 \rangle$, albeit with larger statistical errors due to the fact that the results need to be extrapolated from $q^2 \neq 0$.

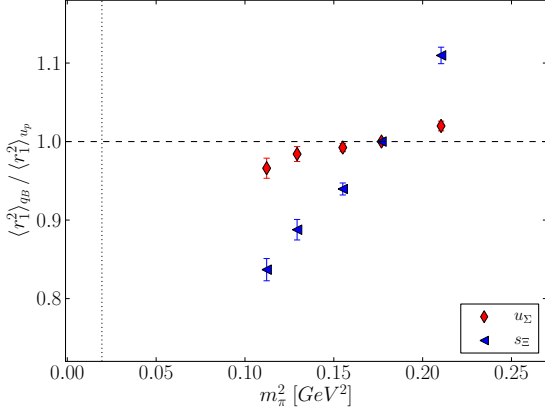


Figure 1: Results for the ratio of the doubly-represented quark's contribution to the Dirac radius of the hyperons, $\langle r_1^2 \rangle_{qB} / \langle r_1^2 \rangle_{u_p}$.

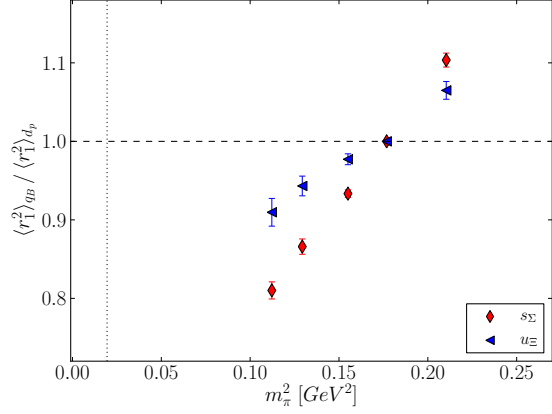


Figure 2: Results for the ratio of the singly-represented quark's contribution to the Dirac radius of the hyperons, $\langle r_1^2 \rangle_{qB} / \langle r_1^2 \rangle_{d_p}$.

4. Hyperon Semi-Leptonic Form Factors

The matrix element for $SU(3)$ -octet baryon semileptonic decays, $B \rightarrow b\ell\nu$, in Euclidean space is given by

$$\langle b(p', s') | V_\mu(x) + A_\mu(x) | B(p, s) \rangle = \bar{u}_b(p', s') (\mathcal{O}_\mu^V(q) + \mathcal{O}_\mu^A(q)) u_B(p, s), \quad (4.1)$$

where the vector and axial-vector transitions are each governed by three form factors, namely the vector (f_1), weak magnetism (f_2), induced scalar (f_3), axial-vector (g_1), weak electricity (g_2) and induced pseudoscalar (g_3)

$$\mathcal{O}_\mu^V(q) = f_1(q^2) \gamma_\mu + f_2(q^2) \sigma_{\mu\nu} \frac{q_\nu}{M_b + M_B} + f_3(q^2) i \frac{q_\mu}{M_b + M_B}, \quad (4.2)$$

$$\mathcal{O}_\mu^A(q) = g_1(q^2) \gamma_\mu \gamma_5 + g_2(q^2) \sigma_{\mu\nu} \frac{q_\nu}{M_b + M_B} \gamma_5 + g_3(q^2) i \frac{q_\mu}{M_b + M_B} \gamma_5. \quad (4.3)$$

The vector and axial-vector currents in Eq. (4.1) are defined as $V_\mu(x) = \bar{u}(x) \gamma_\mu d(x)$ and $A_\mu(x) = \bar{u}(x) \gamma_\mu \gamma_5 d(x)$ for $\Delta S = 0$ decays, and $V_\mu(x) = \bar{u}(x) \gamma_\mu s(x)$ and $A_\mu(x) = \bar{u}(x) \gamma_\mu \gamma_5 s(x)$ for $\Delta S = 1$ decays.

For a lattice calculation of hyperon beta decays, it is useful to define the scalar form factor

$$f_0(q^2) = f_1(q^2) + \frac{q^2}{M_B^2 + M_b^2} f_3(q^2), \quad (4.4)$$

which can be obtained from the divergence of the vector current, $\langle b(p', s') | \partial_\mu V_\mu | B(p, s) \rangle = (M_b - M_B) f_0(q^2) \bar{u}(p', s') u(p, s)$, and the linear combination

$$\tilde{g}_1(q^2) = g_1(q^2) - \frac{M_B - M_b}{M_B + M_b} g_2(q^2). \quad (4.5)$$

The scalar form factor (4.4) can be obtained on the lattice at $q_{\max}^2 = (M_B - M_b)^2$ with high precision from the ratio [11]

$$R(t', t) = \frac{G_4^{Bb}(t', t; \vec{0}, \vec{0}) G_4^{bB}(t', t; \vec{0}, \vec{0})}{G_4^{BB}(t', t; \vec{0}, \vec{0}) G_4^{bb}(t', t; \vec{0}, \vec{0})} \xrightarrow{t, (t'-t) \rightarrow \infty} |f_0(q_{\max}^2)|^2, \quad (4.6)$$

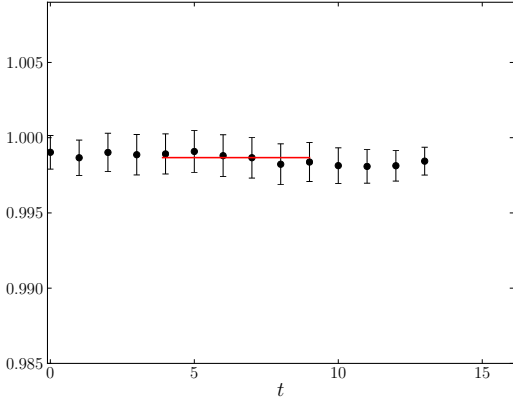


Figure 3: Ratio for $f_0(q_{\max}^2)$, $R(t', t)$, as defined in Eq. (4.6) for ensemble 4 for the $\Sigma^- \rightarrow n\ell\nu$ decay.

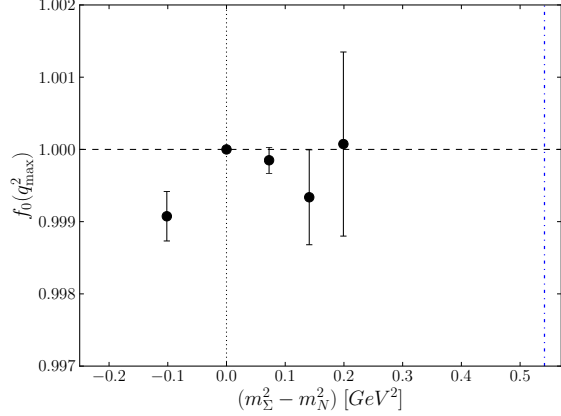


Figure 4: $f_0(q_{\max}^2)$ for $\Sigma^- \rightarrow n\ell\nu$, as a function of the Σ - n mass difference.

where, e.g., $G_4^{Bb}(t', t; \vec{0}, \vec{0})$, is the zero three-momentum lattice three-point function of the fourth component of the vector current, V_4 , inserted at time t between the source baryon, B , located at time $t = 0$ and the sink baryon, b , at time t' . We note that $R(t', t) = 1$ in the $SU(3)_{\text{flavour}}$ symmetric limit, hence any deviations from unity are purely due to $SU(3)_{\text{flavour}}$ symmetry breaking effects.

In Fig. 3 we display our results for $R(t', t)$ for ensemble 4 in Table 1 for the $\Sigma^- \rightarrow n\ell\nu$ decay. Here we see that it is possible to determine $f_0(q_{\max}^2)$ with a high level of accuracy. In order to quantify the size of the $SU(3)_{\text{flavour}}$ symmetry breaking effects in the quantity, in Fig. 4 we show the results for $f_0(q_{\max}^2)$ on each of our ensembles. The results are plotted as a function of $(m_{\Sigma}^2 - m_N^2)$, hence the $SU(3)_{\text{flavour}}$ symmetric limit occurs at zero on the x -axis and is indicated by the vertical dotted line, while the physical mass splitting is indicated by the vertical dot-dashed line. It is obvious from this figure that $f_0(q_{\max}^2)$ is < 1 away from the $SU(3)_{\text{flavour}}$ symmetric limit and that the deviation from unity increases as we move further away from the $SU(3)_{\text{flavour}}$ symmetric limit. We find the same qualitative behaviour in our results for the $\Xi^0 \rightarrow \Sigma^+ \ell\nu$ decay and these findings are in agreement with earlier lattice results [6, 7].

The next step is to determine the full q^2 -dependence of $f_0(q^2)$ and interpolate the results to $q^2 = 0$ to obtain a value for $f_1(0) = f_0(0)$. The procedure for doing this has been described in detail in [6], and this is the next step in our work which will be completed soon.

The other quantity that we need to calculate before we can determine $|V_{us}|$ from Eq. (1.1) is $g_1(0)/f_1(0)$. As pointed out in [6], this can also be determined from considering appropriate ratios of two- and three-point functions. At q_{\max}^2 , it is possible to determine the ratio $\tilde{g}_1(q_{\max}^2)/f_0(q_{\max}^2)$ from the following ratio of three-point functions

$$\tilde{R}(t', t) = \frac{\text{Im}(A_3^{Bb}(t', t; \vec{0}, \vec{0}))}{\text{Re}(V_4^{Bb}(t', t; \vec{0}, \vec{0}))} \xrightarrow{t, (t'-t) \rightarrow \infty} \frac{g_1(q_{\max}^2) + \frac{M_B - M_b}{M_B + M_b} g_2(q_{\max}^2)}{f_1(q_{\max}^2) + \frac{M_B - M_b}{M_B + M_b} f_3(q_{\max}^2)} \equiv \frac{\tilde{g}_1(q_{\max}^2)}{f_0(q_{\max}^2)}. \quad (4.7)$$

We show in Fig. 5 $\tilde{R}(t', t)$ from ensemble 1 where we see again the excellent accuracy with which the ratio can be determined. The dependence of this ratio on the size of the $SU(3)_{\text{flavour}}$ symmetry breaking is seen in Fig. 6.

Once again, this is only the first step in calculating $g_1(0)/f_1(0)$ and so we must now subtract the second terms in both numerator and denominator in Eq. (4.7) in order to obtain $g_1(q_{\max}^2)/f_1(q_{\max}^2)$.

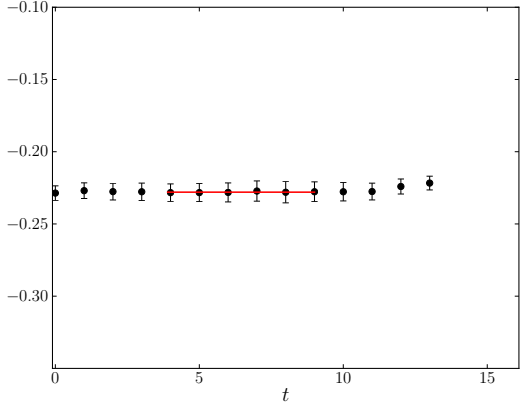


Figure 5: Ratio for $\tilde{g}_1(q_{\max}^2)/f_0(q_{\max}^2)$ as defined in Eq. (4.7) for ensemble 1 for the $\Sigma^- \rightarrow n\ell\nu$ decay.

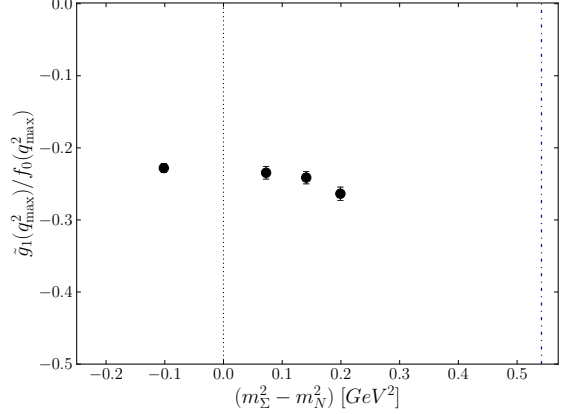


Figure 6: $\tilde{g}_1(q_{\max}^2)/f_0(q_{\max}^2)$ for $\Sigma^- \rightarrow n\ell\nu$, as a function of the Σ - n mass difference.

We then need to map out the q^2 -dependence of $g_1(q^2)/f_1(q^2)$ which will then enable us to interpolate to $q^2 = 0$. This will be completed soon.

5. Conclusions

We have presented preliminary results from the QCDSF/UKQCD collaboration for the electromagnetic semileptonic decay form factors of the $SU(3)$ baryon octet.

Our results for the individual quark contributions to the Dirac radii of the hyperons show that the $u(d)$ -quark is more broadly distributed in the proton (neutron) than in the $\Sigma^{+(-)}$, while the s -quark in the Ξ is the least broadly distributed of the doubly-represented quarks. Similarly for the singly-represented quarks, we find that the $d(u)$ -quark is more broadly distributed in the proton (neutron) than in the $\Xi^{-(0)}$, while the s -quark in the Σ is the least broadly distributed.

For the hyperon semileptonic form factors, we have only performed the first stage of the analysis by computing the appropriate form factors at q_{\max}^2 . Our results are encouraging and show a similar quark mass behaviour as earlier quenched [6] and $N_f = 2$ [7] results.

Acknowledgements

The numerical calculations have been performed on the apeNEXT at NIC/DESY (Zeuthen, Germany), the IBM BlueGeneL at EPCC (Edinburgh, UK), the BlueGeneL and P at NIC (Jülich, Germany), the SGI ICE 8200 at HLRN (Berlin-Hannover, Germany) and the JSCC (Moscow, Russia). We thank all institutions. We have made use of the Chroma software suite [12], employing the SSE optimised Dslash code [13], while our Bluegene codes were optimised using Bagel [14]. This work has been supported in part by the DFG (SFB/TR 55, Hadron Physics from Lattice QCD) and the European Union under grants 238353 (ITN STRONGnet) and 227431 (HadronPhysics2). JZ is supported through the UK's STFC Advanced Fellowship Programme under contract number ST/F009658/1.

References

- [1] Ph. Hägler, “*Hadron structure from lattice quantum chromodynamics*,” Phys. Rept. **490** (2010) 49 [arXiv:0912.5483 [hep-lat]].
- [2] S. Boinapalli *et al.*, “*Precision electromagnetic structure of octet baryons in the chiral regime*,” Phys. Rev. **D74** (2006) 093005 [hep-lat/0604022].
- [3] H. -W. Lin and K. Orginos, “*Strange Baryon Electromagnetic Form Factors and SU(3) Flavor Symmetry Breaking*,” Phys. Rev. **D79** (2009) 074507 [arXiv:0812.4456 [hep-lat]].
- [4] N. Cabibbo, E. C. Swallow and R. Winston, “*Semileptonic hyperon decays*,” Ann. Rev. Nucl. Part. Sci. **53** (2003) 39 [arXiv:hep-ph/0307298].
- [5] J. M. Gaillard and G. Sauvage, “*Hyperon Beta Decays*,” Ann. Rev. Nucl. Part. Sci. **34** (1984) 351.
- [6] D. Guadagnoli, V. Lubicz, M. Papinutto and S. Simula, “*First lattice QCD study of the Sigma- \rightarrow n axial and vector form factors with SU(3) breaking corrections*,” Nucl. Phys. B **761** (2007) 63 [arXiv:hep-ph/0606181].
- [7] S. Sasaki and T. Yamazaki, “*Lattice study of flavor SU(3) breaking in hyperon beta decay*,” Phys. Rev. **D79** (2009) 074508 [arXiv:0811.1406 [hep-ph]].
- [8] N. Cundy *et al.* [QCDSF/UKQCD Collaboration], “*Non-perturbative improvement of stout-smearred three flavour clover fermions*,” Phys. Rev. **D79** (2009) 094507 [arXiv:0901.3302 [hep-lat]].
- [9] W. Bietenholz *et al.* [QCDSF/UKQCD Collaboration], “*Tuning the strange quark mass in lattice simulations*,” Phys. Lett. **B690** (2010) 436 [arXiv:1003.1114 [hep-lat]].
- [10] D. B. Leinweber, “*Quark contributions to baryon magnetic moments in full, quenched and partially quenched QCD*,” Phys. Rev. **D69** (2004) 014005 [hep-lat/0211017].
- [11] S. Hashimoto *et al.*, “*Lattice QCD calculation of anti-B \rightarrow D lepton anti-neutrino decay form-factors at zero recoil*,” Phys. Rev. **D61** (1999) 014502 [hep-ph/9906376].
- [12] R. G. Edwards and B. Joó, “*The Chroma software system for lattice QCD*,” Nucl. Phys. Proc. Suppl. **140** (2005) 832 [hep-lat/0409003].
- [13] C. McClendon, “*Optimized Lattice QCD Kernels for a Pentium 4 Cluster*,” Jlab preprint, JLAB-THY-01-29, http://www.jlab.org/~edwards/qcdapi/reports/dslash_p4.pdf
- [14] P. A. Boyle, “*The BAGEL assembler generation library*,” Comp. Phys. Comm. **180**, (2009) 2739.